Bio-Medical Materials and Engineering 34 (2023) 331–344
DOI 10.3233/BME-221450
IOS Press

An extracellular matrix hydrogel from porcine urinary bladder for tissue engineering: *In vitro* and *in vivo* analyses

German Jiménez-Gastélum[a], Rosalío Ramos-Payán[b], Jorge López-Gutierrez[a], Alfredo Ayala-Ham[a,c], Erika Silva-Benítez[c], Mercedes Bermúdez[d], José Geovanni Romero-Quintana[b], Guzman Sanchez-Schmitz[e] and Maribel Aguilar-Medina[b,*]

[a]*Faculty of Biology, Autonomous University of Sinaloa, Culiacan, Mexico*
[b]*Faculty of Biological and Chemical Sciences, Autonomous University of Sinaloa, Culiacan, Mexico*
[c]*Faculty of Odontology, Autonomous University of Sinaloa, Culiacan, Mexico*
[d]*Faculty of Odontology, Autonomous University of Chihuahua, Chihuahua, Mexico*
[e]*Boston Children's Hospital and Harvard Medical School, Harvard University, Boston, MA, USA*

Received 7 June 2022
Accepted 14 December 2022

Abstract.
BACKGROUND: The necessity to manufacture scaffolds with superior capabilities of biocompatibility and biodegradability has led to the production of extracellular matrix (ECM) scaffolds. Among their advantages, they allow better cell colonization, which enables its successful integration into the hosted tissue, surrounding the area to be repaired and their formulations facilitate placing it into irregular shapes. The ECM from porcine urinary bladder (pUBM) comprises proteins, proteoglycans and glycosaminoglycans which provide support and enable signals to the cells. These properties make it an excellent option to produce hydrogels that can be used in regenerative medicine.
OBJECTIVE: The goal of this study was to assess the biocompatibility of an ECM hydrogel derived from the porcine urinary bladder (pUBMh) *in vitro* using fibroblasts, macrophages, and adipose-derived mesenchymal stem cells (AD-MCSs), as well as biocompatibility *in vivo* using Wistar rats.
METHODS: Effects upon cells proliferation/viability was measured using MTT assay, cytotoxic effects were analyzed by quantifying lactate dehydrogenase release and the Live/Dead Cell Imaging assay. Macrophage activation was assessed by quantification of IL-6, IL-10, IL-12p70, MCP-1, and TNF-α using a microsphere-based cytometric bead array. For *in vivo* analysis, Wistar rats were inoculated into the dorsal sub-dermis with pUBMh. The specimens were sacrificed at 24 h after inoculation for histological study.
RESULTS: The pUBMh obtained showed good consistency and absence of cell debris. The biocompatibility tests *in vitro* revealed that the pUBMh promoted cell proliferation and it is not cytotoxic on the three tested cell lines and induces the production of pro-inflammatory cytokines on macrophages, mainly TNF-α and MCP-1. *In vivo*, pUBMh exhibited fibroblast-like cell recruitment, without tissue damage or inflammation.
CONCLUSION: The results show that pUBMh allows cell proliferation without cytotoxic effects and can be considered an excellent biomaterial for tissue engineering.

Keywords: Urinary bladder extracellular matrix, hydrogel, biological scaffolds, biocompatibility

*Corresponding author: Maribel Aguilar-Medina, PhD, Faculty of Chemical and Biological Sciences, Autonomous University of Sinaloa, Josefa Ortiz de Domínguez s/n y Avenida de las Américas, 80010 Culiacán, Sinaloa, Mexico. E-mail: maribelaguilar@uas.edu.mx.

1. Introduction

The need to manufacture biomaterials with superior biocompatibility and biodegradability capacities for tissue regeneration is increasing [1]. Damaged tissue requires three factors to achieve regeneration, cells, scaffolds, and biosignals [2]. The scaffolds based on natural extracellular matrix (ECM) confer mechanical properties, stimulates the migration of cell populations, regulate biosignals that enhances cell growth and differentiation of mesenchymal stem cells (MSCs) [3–5], achieving synergy capable of restoring the functions of the affected or diseased tissues and organs [6–10]. The specific elements of ECM consist of collagens, elastins (primary structural elements, the most abundant), and noncollagenous proteins such as fibronectin, vitronectin, osteopontin, glycosaminoglycans (GAGs), and growth factors [11]. GAGs (heparans, dermatans, chondroitins, and hyaluronans) act as crosslinkers and can store growth factors, and cytokines/chemokines due to their negative charge and binding sites for specific proteins [11].

ECM scaffolds can be obtained from different tissues such as the pancreas, skin, bone, small intestine, liver, and urinary bladder, among others [12]. In this context, ECM hydrogel scaffolds are considered an alternative due to their ability to fill an irregularly shaped space and have the advantage of being injectable, which facilitates access to areas with minimal surgical intervention [13]. Hydrogels can be prepared from various sources of ECM through decellularized tissues, pepsin solubilization process, and then polymerized under physiological conditions [14–16]. The solubilized or polymerized ECM has also been evaluated with different cells, determining cell biocompatibility *in vitro* and showing various effects on cell metabolism and macrophage stimulation [17,18]. It has also been reported that hydrogels can improve the recruitment of inflammatory cells in injured areas and stimulate macrophages and fibroblasts in the wound healing process [19,20]. On the other hand, the preparation of hydrogel scaffolds include the exposure to trypsin or detergent are typical used for decellularization [13,21,22] and enzymatic digestion, commonly with pepsin, is used for solubilization.

The hydrogel is physical and chemical cross-linked hydrophilic scaffold to which biological molecules can be conjugated, creating a 3D environment almost identical to the native ECM [23]. Hydrogels are defined as highly hydrated polymeric materials (>30% water by weight). ECM hydrogels expand their use because due to their easy handling, they allow the infiltrated being to show great capacity to fill an irregularly shaped space, preserving the bioactivity of the native matrix [18].

The ECM derived from the porcine urinary bladder (pUBM) enhances the migration of specific progenitor cells, incorporates fully into wounds, and promotes the formation of site suitable tissue through constructive modeling with a parallel anti-inflammatory response [24], making it a substrate for cell attachment, differentiation, and proliferation [25]. Besides, pUBM, in the form of particulate or patches, has been broadly investigated in preclinical studies about tissue remodeling for the urethra, larynx, esophagus, and heart, and lately, it has been investigated in the form of a hydrogel. Nevertheless, given the lack of standard protocol for the preparation of hydrogel scaffolds, this work aimed to evaluate the *in vitro* and *in vivo* biocompatibility of a pUBM hydrogel (pUBMh).

2. Materials and methods

2.1. Preparation of pUBMh

Porcine urinary bladders were harvested from Chester White market pigs (Fapsa y Asociados, Sinaloa, Mexico), quality certified ISO 9001–2008. Decellularization protocol was followed according to Silva

et al., with some modifications [26]. The bladders were decontaminated by rinsing in 10% iodine solution and transported in phosphate-buffered saline (PBS) with 100 IU/mL penicillin and 100 mg/mL streptomycin. A sample of complete urinary bladder was taken as a control. First, the inner layer (submucosa) of the tissue was separated from the muscle by mechanical delamination and then stirred in 0.25% trypsin solution overnight. Histological analysis was developed to evaluate cell removal, finally, to prepare pUBM pre-gel the remnants were frozen, lyophilized, and milled to create a powder and finally digested with pepsin for solubilization. Then, the pUBM-hydrogel was obtained by mixing the pUBM pre-gel with PBS 1× and NaOH (1 M) allowing it to gel for 30 min at 37 °C, and then it was stored at −20 °C. To determine cellular content, samples before and after trypsin digestion were fixed in 10% formalin, embedded in paraffin, and cut into 7-µm sections. The slices were stained with H&E and images were taken at 10× and 40× using a TCS SP8 microscope system (Leica, Germany).

2.2. *Cell culture conditions for biocompatibility assays*

3 different cells lines were used to determine the biocompatibility of hydrogels *in vitro*, RAW 264.7 murine macrophage (TIB-71, ATCC), NIH/3T3 murine fibroblast (CCL-92, ATCC), and human Adipose-Derived Mesenchymal Stem Cells (AD-MCSs, PCS-500-011, ATCC) were grown with Dulbecco's Modified Eagle's Medium (DMEM, GIBCO, USA) supplemented with 10% heat-inactivated fetal bovine serum (FBS, GIBCO) and Penicillin-Streptomycin (10,000 U/mL) (Gibco) at 37 °C with 5% CO_2. Cells of the third passage were used at 80% of cell confluence for experiments. Cells were harvested using 0.25% trypsin-EDTA (GIBCO).

2.3. *pUBMh extracts preparation for biocompatibility assays*

A conditioned medium for evaluation of cell biocompatibility *in vitro* was prepared from pUBMh. First, 1 ml of hydrogel (20 mg/ml) and 9 ml of supplemented medium were placed with 0.05 mm glass beads in a tissue disruptor for 1 min at maximum speed (Disruptor Genie, Scientific Industries, USA) and incubated at 37 °C with constant shaking for 24 h. Finally, the conditioned medium was centrifuged at 13,000 rpm and the recovered supernatants were filtrated with a 0.22 µm membrane (Cytiva Whatman, USA). This cultured medium was used for LDH, MTT, live/dead, and cytokine expression assays.

2.4. *Cellular proliferation assay*

Cell proliferation/viability was measured using the MTT assay (CellTiter 96 NON-Radioactive Cell Proliferation Assay, PROMEGA, USA). The cells were cultured in 96-well plates with supplemented medium DMEM placing 7.5×10^3 cells/well. At 24 h media were replaced and cells were exposed to the conditioned medium during 24, 48, and 72 h, and after incubation measures were performed. Briefly, in 100 µL of culture medium cells were incubated with 15 µl of tetrazolium salt solution for 2 h. The violet formazan salts were then dissolved by adding 100 µl of stop solution. The optical density (OD) was measured at 570 nm in a microplate reader.

2.5. *Cytotoxicity of pUBMh assay*

To evaluate the pUBMh cell lysis effect, cells were cultured in 96-well plates with supplemented medium DMEM at a density of 15×10^3 cells/well. At 24 h media were replaced by conditioned

medium and after 24 h cytotoxicity was measured by quantifying lactate dehydrogenase (LDH) release in supernatants by colorimetric assay following the manufacturer's instructions (LDH Cytotoxicity assay, Sigma-Aldrich, USA). OD was measured at 490 nm in a microplate reader.

2.6. Live/dead assay

Live/Dead assay was performed to evaluate cell membrane integrity using thiazole orange and propidium iodide. Cells were seeded in 24-well plates with supplemented medium DMEM at a density of 10×10^4 cells/well. At 24 h media were replaced, and cells were exposed to conditioned medium for 24 h, and then incubated with thiazole orange 84 nM (Sigma-Aldrich) and propidium iodide 4.3 μM (Sigma-Aldrich) for 5 min at room temperature. The samples were then examined using a TCS SP8 microscope system at 40×. Relative fluorescence units (RFU) were measured, and percentages for cell viability were obtained.

2.7. Cytokine expression analysis

For evaluation of macrophage response to pUBMh, RAW 264.7 macrophages were cultured into a 24 well plate with supplemented medium DMEM placing 5×10^5 cells/well. At 24 h media were replaced by conditioned medium and after 24 h cytokine expression was evaluated in supernatants by measuring in supernatants concentrations of IL-6, IL-10, IL-12p70, MCP-1, and TNF-α, using a microsphere-based (CBAs) according to manufacturer's instructions (BD Bioscience, USA). Data were acquired using Accuri C6 flow cytometer and quantification with FCAP Array software v3.0 (BD Bioscience). LPSs were used to treat cells as a positive control.

2.8. In vivo biocompatibility

To determine *in vivo* biocompatibility of pUBMh a subcutaneous inoculation model was employed. 3-month-old Wistar rats (250–300 g) were anesthetized by placing 1 μL of sedative cocktail (70% Ketamine, 15% Xylazine, 15% Injectable water) per mg of weight, intramuscularly. Briefly, the back was shaved and disinfected with 70% alcohol, then 200 μl of pUBMh, positive control (chloroform) or negative control (PBS 1X) were inoculated into the dorsal region, taking as reference the midline of the back. The specimens were sacrificed at 24 h and immediately 2 in diameter of tissue were cut around the inoculation area, the tissue was fixed with 1X Phosphate Buffered Saline (PBS) with 4% paraformaldehyde and histological evaluations were carried out to observe the inflammatory reaction. Ethical issues use of animals was approved according to the signed statement of the Animal Ethics Committee of the Faculty of Biological and Chemical Sciences, University Autonomy of Sinaloa.

2.9. Histological section and H&E staining

The complete urinary bladder, pUBM, and the implants harvested were fixed in 10% formalin, embedded in paraffin, and cut into 7-μm sections. The sample slices were stained with H&E. Images were taken using a TCS SP8 microscope system.

2.10. Statistical analysis

Experiments were performed three times by triplicate, and results were represented as mean ± SD. ANOVA and Dunnet's post hoc test were used for 3 or more parametric variables. $p < 0.05$ was considered statistically significant.

3. Results and discussion

3.1. pUBMh obtained is a cell-free scaffold

ECM material in the form of hydrogel has broad potential *in vitro* and *in vivo* application. According to Saldin et al., the prerequisites for preparing ECM hydrogel are that the tissues must be effectively decellularized to retain the ECM scaffold and the resulting substratum should be able to be enzymatically solubilized and neutralized into hydrogel form under appropriate physiological conditions [13]. Thus, after performing the mechanical delamination of the urothelia, we continued with the enzymatic digestion using trypsin/EDTA. We found through images and analysis of the section stained with H&E the removal of cellular components (Fig. 1). Native bladder ECM free of trypsin treatment was used as control showing cellular content with defined nuclei (Fig. 1A and B, black arrows). Besides, we corroborate that the methodology by Silva et al., with some modifications [26], is sufficient to obtain a cell-free scaffold since the absence of nuclei and the presence of acellular gaps after trypsin treatment (Fig. 1C and D, red arrows).

3.2. Cell biocompatibility with pUBMh extracts

The effects on cell proliferation of the ECM extracts were evaluated by an MTT assay that measures the metabolic activity of the cells. All cell lines treated with pUBMh presented a higher metabolic activity than the control group (DMEM) at 24, 48 and 72 h, showing greater cell viability (Fig. 2D, E and F). Interestingly, all three cell lines showed increased proliferation at 48 h compared to the DMEM control, and this behavior continued to increase up to 72 h. Proliferation in different cell lines has been shown to be positively affected by the presence of demineralized and decellularized bone extracellular matrix hydrogels [27,28]. pUBMh is manufactured as a cellular component-free scaffold facilitating rapid degradation and prompt replacement with site-appropriate functional host tissue and cells. It has been shown that the presence of cell debris has been related to inflammatory cells and macrophages with the M1 polarization profile [29]. Decellularized ECM is also known to be source-dependent, as those derived from skeletal muscle, dermis, colon, brain, and urinary bladder can reduce macrophage MTT metabolism by up to 50%, whereas ECM from the submucosa of the small intestine, esophagus, and liver does not affect cellular metabolism [17]. However, in this study, we found that pUBMh induced upregulated metabolic activity of macrophages without promoting cell lysis or interfering with cell proliferation. This could be due the polarization of macrophages from M1 to M2 that is induced by the pUBM as it has been previously described by Page et al. [30]. Therapies promoting increased M2 or decreased M1 macrophage polarization in the later stages of wound healing are adequate at enhancing wound healing even in diabetic patients [31,32]. Nevertheless, more studies need to be developed to demonstrate the macrophages polarization in our model.

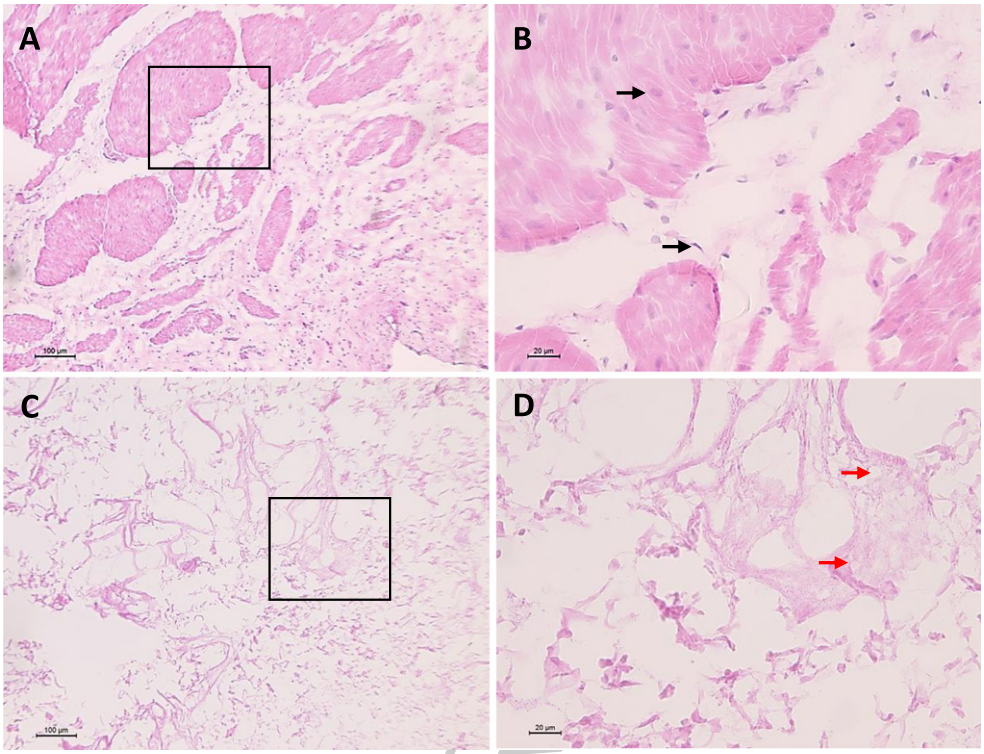

Fig. 1. Porcine UBM decellularization. pUBM shows cellular content before treatment with trypsin/EDTA, at 10× (A) and 40× (B) magnification (black arrows). Free-cell regions with the absence of nuclei and the presence of acellular lacunae (red arrows) are evident in pUBM after trypsin/EDTA treatment, at 10× (C) and 40× (D) magnification (red arrows). Histological slides (H&E), scale bar 100 µm.

Fibroblasts are cells regularly used for exploring biocompatibility on ECM-based material [33]. In our case, a marked induction in proliferation was observed after 48 h, maintaining this behavior until 72 h, which is the expected, since this behavior is key in this type of cell, as they are responsible for maintenance of the stroma by synthesizing growth factors and cytokines responsible for cell recruitment, essential for tissue regeneration [34]. Besides, recent cell therapies are based on the use of ECM, cryopreserved placental tissue, and fibroblasts to induce tissue regeneration [35]. Regarding AD-MCSs cells, our results showed a slightly higher behavior in proliferation after 48 h, becoming potentiated at 72 h. This delay could be caused by culture conditions since this cells grow better in mesenchymal stem cell basal medium (MSCBM) and supplemented with 2% FBS, 5 ng/mL rh FGF basic, 5 ng/mL rh FGF acidic, 5 ng/mL rh EGF, 2.4 mM L-Alanyl-L-Glutamine [36]. It has been shown that failure of tissue regeneration can lead to fibrosis orchestrated by chronic inflammation, leading to nonfunctional tissue or damaged neoformation [37] but, when MSCs cells are placed, they could greatly reduce inflammatory conditions, since they synthesize anti-inflammatory cytokines and proangiogenic factors [38]. For instance, the hepatocyte growth factor increases the expression of matrix metalloproteinases 1, 3 and 13, thus favoring the remodeling of ECM, as well as the low expression of TGF-β1, COL-1 and COL-3 in hepatocytes [39]. In our study we evaluated these types of cells as they are closely linked in tissue regeneration processes. The combination of all the elements creates an ideal niche, given their intimate interaction which minimizes the undesired effects of healing damaged tissue, promoting optimal conditions [40].

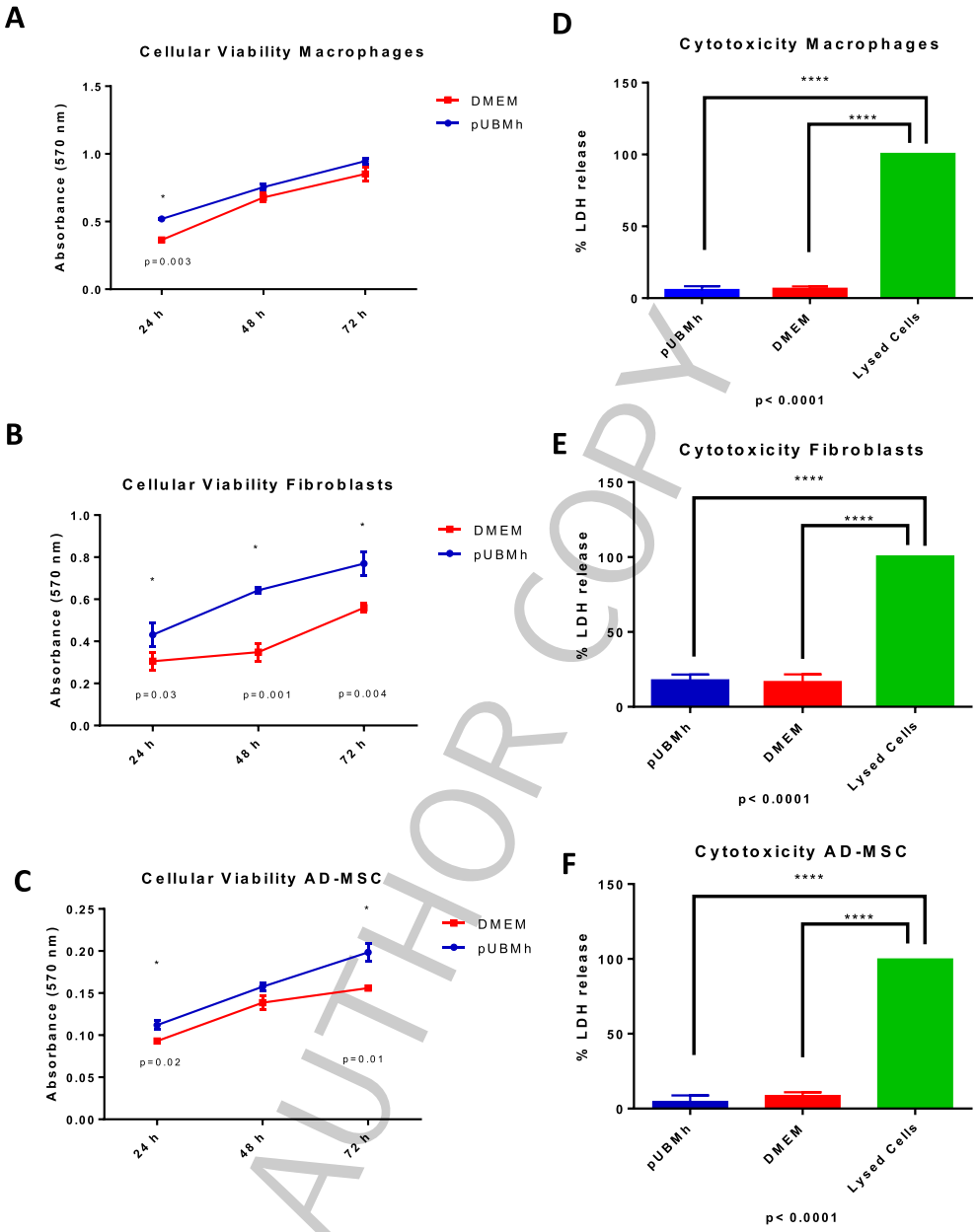

Fig. 2. To analyze proliferation induced by pUBMh extract, MTT assay was developed in macrophages (A), fibroblasts (B) and AD-MCSs (C). All cell lines showed increased cell viability from 24 to 72 h with both, pUBMh and DMEM. To evaluate cytotoxicity, a total of 4 mg/mL were incubated in contact with macrophages (D), fibroblasts (E) and AD-MCSs (F). Interestingly, we found that LDH release patterns were similar among the different cell lines when compared to the DMEM group (pUBMh versus DMEM) and statistical differences were only found when OD was compared to LDH release of control (lysed cell, $p < 0.0001$).

When working with materials from decellularized scaffolds, the cytotoxicity should be studied given their immunogenicity and the toxicity of the residual chemicals from the decellularization reagents [41].

For this reason, the release of LDH from lysis was measured (Fig. 2A, B and C) Optical Densities (OD) were higher in macrophages (0.135 ± 0.08 versus 0.102 ± 0.04 OD) compared to fibroblasts (0.072 ± 0.03 versus 0.067 ± 0.02 OD) and MCS (0.048 ± 0.02 versus 0.062 ± 0.01 OD). Statistical differences were only found when OD was compared with LDH release from the control (lysed cell, $p < 0.0001$). Furthermore, the live/dead assay allowed to identify that there is no disruption in the integrity of the cell membrane in any of the cells treated with pUBMh. Additionally, fibroblasts and MSCs showed a typical cell morphology. The live cell percentages of macrophages (92.8% vs. 93.5%), fibroblasts (93.1% versus 92.9%), and MSCs (96.4% versus 95.8%) revealed cells free of membrane damage and the percentage of living cells was similar to that of the control group (Fig. 3A, B and C). In addition, cell morphology was not compromised after exposure to the soluble extract (Fig. 3E, D, and F) demonstrating that pUBMh is not cytotoxic to any of the cell lines, on the contrary, induced an upregulated metabolic activity of fibroblasts, macrophages and MSCs without promoting cell lysis or interfere on cell proliferation.

3.3. pUBMh stimulates IL-12, TNF-α and MCP-1 pro-inflammatory cytokines production in macrophages

Evaluating the cytokine profile in macrophages is of great relevance to obtain information on the impact of pUBMh on the processes of inflammation and cell recruitment. Our results showed that according to the proinflammatory cytokine expression profile, pUBMh promotes polarization towards M1, since after exposure to the hydrogel extract in macrophages, we found an increase in the proinflammatory cytokine IL12 (31.18 ± 25.68 versus 14.10 ± 0.37 pg/mL) (Fig. 4C) and TNF-α (1357.99 ± 27.29 versus 247.37 ± 18.91 pg/mL) (Fig. 4B). The chemotactic cytokine MCP-1 was also increased (414.70 ± 16.38 versus 118.96 ± 6.40 pg/mL, $p = 0.000$) (Fig. 4D). On the other hand, the concentration of IL-6 (25.57 ± 5.26 versus 16.07 ± 7.39 pg/mL) and the concentration of the anti-inflammatory cytokine, IL-10 (43.22 ± 2.76 versus 40.39 ± 4.55 pg/ml) (Fig. 4C and E) were not altered by exposure to pUBMh hydrogel extract. Other authors have reported that urinary bladder matrix can promote the M2 phenotype, expressing surface markers of Fizz1 and CD206 with low levels of M1-like iNOS expression [17]. Under normal physiological conditions, damage or injury promotes inflammation to increase blood flow and extravasation, inducing accumulation of interstitial fluid, leukocytes, recruitment of inflammatory mediators, and upregulation of proinflammatory cytokines, commonly IL-1β and TNF-α [42,43]. There are reports focused on the regeneration of liver tissue where they observe a dose-dependent increase in mitotic rates, when exposed to TNF-α [44,45]. It is also known that IL-6 increases in liver tissue regeneration, since TNF-α orchestrates the synthesis of IL-6 [46], this suggests that the pUBMh hydrogel promotes proinflammatory cytokines to initiate a regenerative process. On the other hand, it has been shown that MCP-1 is a chemotactic cytokine that actively induces angiogenesis and vasculogenesis process [47,48], by regulating VEGF and HIF-α through the activation of the transcription factor ETS-1 [49]. Our results allow us to suggest that the stimulation of pUBMh promotes angiogenesis through the activation of secondary factors due to the effect of MCP-1. Li et al. showed that IL-12 induces a significantly faster onset and higher metabolic activity of the inflammatory response in wounded skin during the early moments of wound healing [50]. Immediately after injury, the macrophage reaches the injury site via diapedesis, aiding the IL-12-mediated T cell response [51]. This demonstrates that each of the cytokines expressed in this study are involved in early stages of inflammation. which would induce an adequate tissue regeneration pathway. However, more experiments are required to confirm these possible mechanisms.

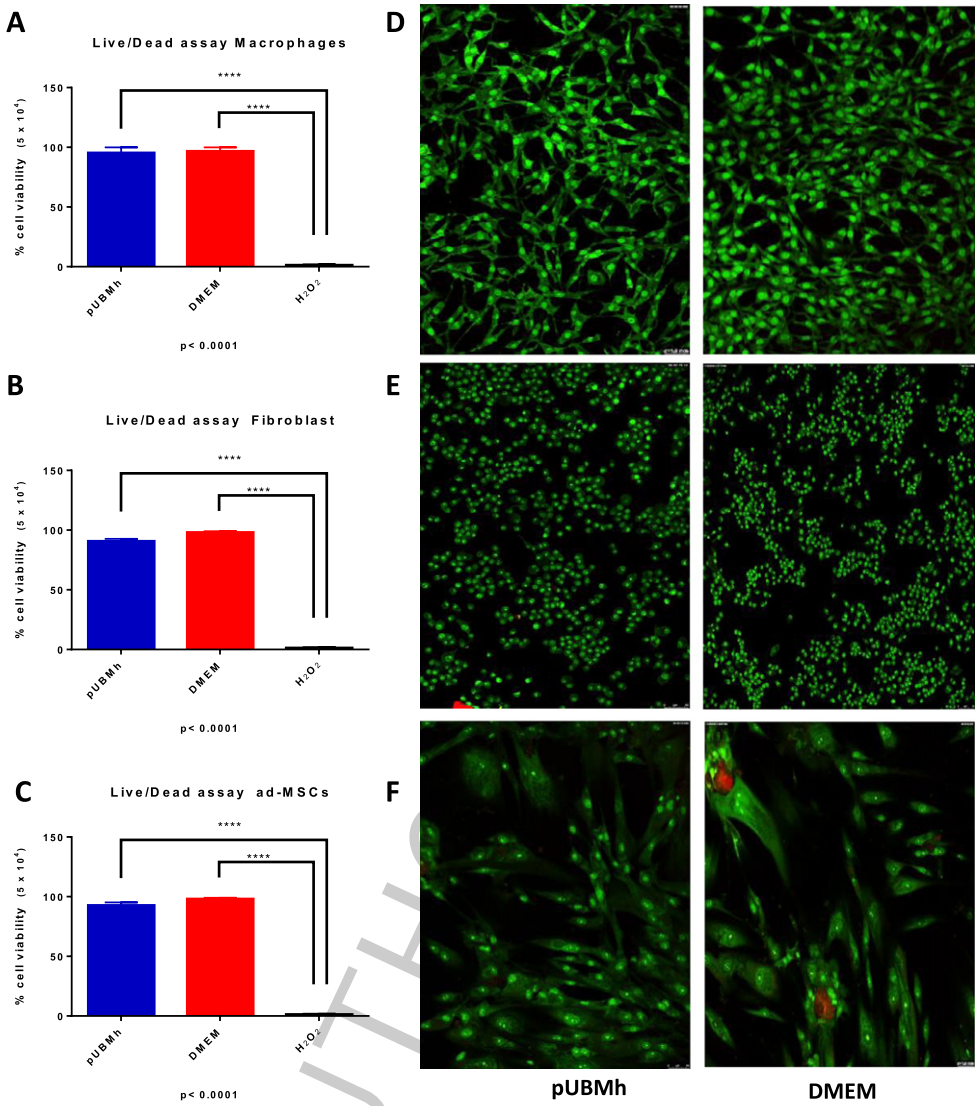

Fig. 3. Cell viability of macrophages, fibroblasts and AD-MCSs in contact with pUBMh extract was evaluated using LIFE/DEATH Cell Viability Assay by confocal microscopy. Cell viability did not show significant differences (pUBMh versus DMEM) and differences were only found when compared to the positive control of dead (A, B and C) demonstrating that pUBMh is biocompatible with multiple cell lines. Moreover, cellular morphology was not compromised after soluble extract exposure as was confirmed by confocal microscopy (D, E, and F).

3.4. pUBMh acts as a scaffold allowing host fibroblastic-like cells colonization in vivo

For *in vivo* biocompatibility, a model of subcutaneous transplantation in mice was used to investigate their capability for cellularization, vascularization and immunoregulatory effect of pUBMh. It was possible to observe that the pUBMh promotes the recruitment of cells, including macrophages, lymphoblastic and fibroblastic-like cells with absence of inflammatory cells (Figs 5B and C). This type of behavior have been seen using hydrogel derived from the extracellular matrix of the human umbilical

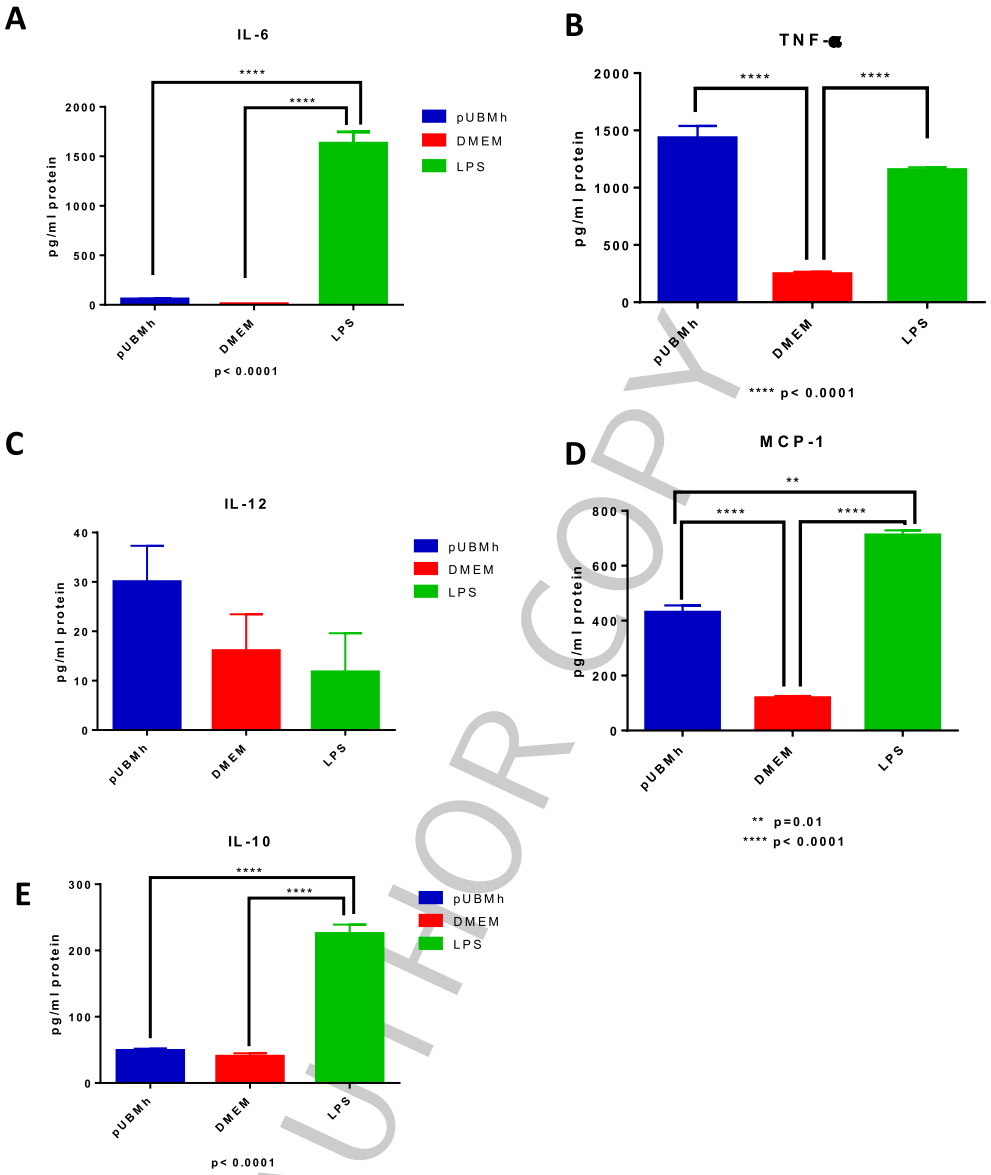

Fig. 4. Proinflammatory cytokine production in macrophages exposed to pUBMh extract. We found an increase in pro-inflammatory cytokines TNF-α (B), IL-12 (C) and for chemotactic cytokine MCP-1(D). On the other hand, IL-6 and anti-inflammatory cytokine IL-10 (A and E) concentrations were not altered by pUBMh extract exposure.

cord, observing an improvement in the colonization of host cells in the implantation zone [52]. Our results are in agreement with Wue et al. and showed that hydrogels derived from natural ECM molecules have numerous potential advantages for therapeutic applications including strong bioactive substances to supply vital microenvironment, simple to deliver via injections to fill irregular and large defects, and no risk of immunologic rejection when applied during allografting [53]. Besides, it has been shown that porcine urinary bladder matrix preserve multiple intrinsic growth factors, including TGF-β, VEGF, PGF, BMP4 and FGF, which directly impact wound healing [54]. Besides, antimicrobial properties of pUBM to

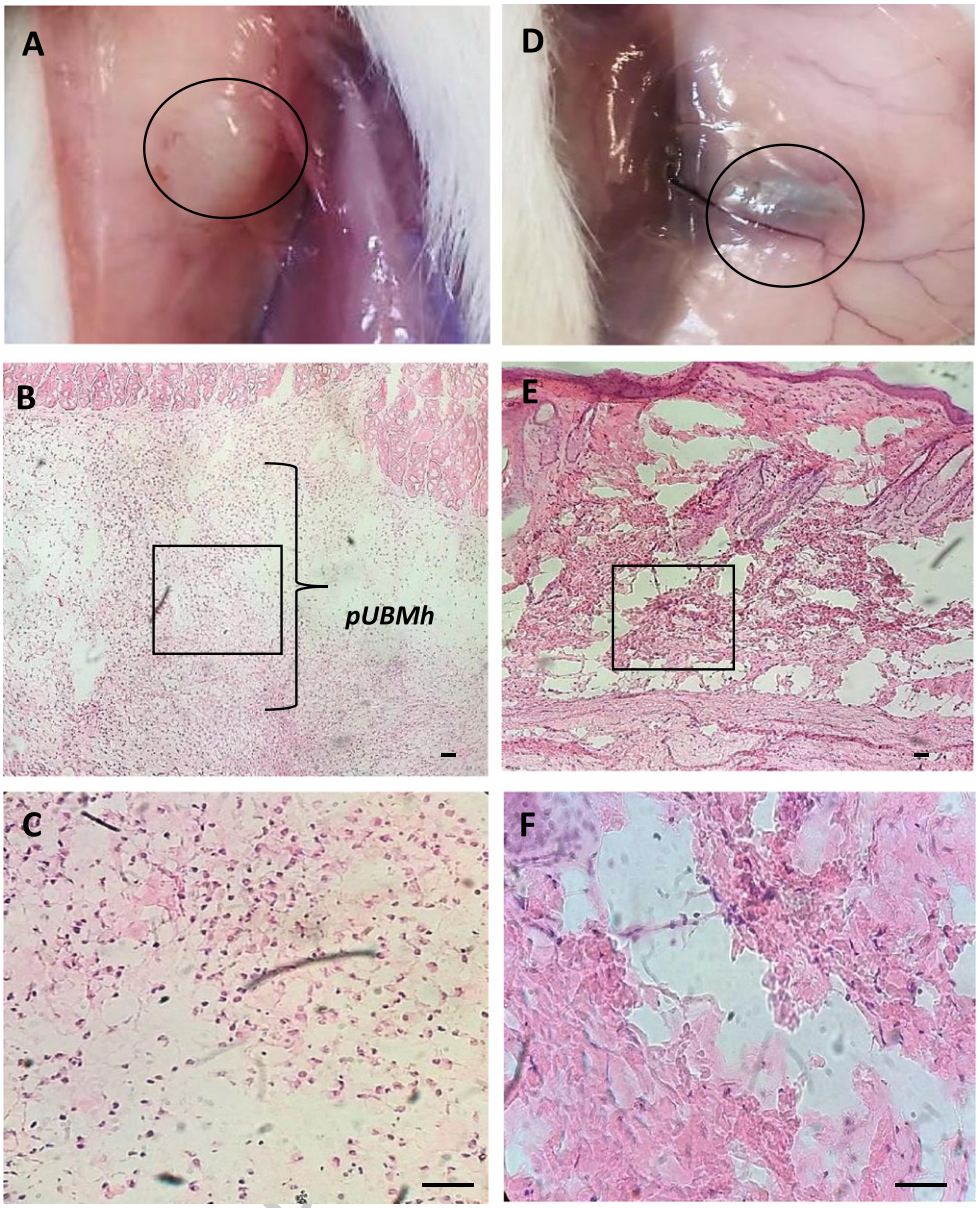

Fig. 5. *In vivo* biocompatibility of pUBMh. 24 h after subcutaneous injection in the dorsal region of pUBMh (A, B and C) and chloroform (D, E and F) as damage control, reaction tissue was observed. pUBMh remains stable in a well-defined area (black circle), without any dermal abnormalities (A). At 10×, low cellularity was observed within the material (B). Higher magnification (40×) (black box) showed the pUBMh fibrillar structure, with few polymorphonuclear and fibroblast-like cells present (C). In contrast, the chloroform injection caused severe damage by inducing a hematoma (D). At 10× the severe inflammatory infiltrate can be seen, as well as loss of dense connective tissue cohesion (E) and at 40× magnification the presence of epithelioid-type macrophages interspersed with fibroblastoid-type cells (F). Scale bar 50 µm.

Staphylococcus aureus and *Escherichia coli* enhance healthy functional tissue regeneration with increased chemotactic activity [55].

4. Conclusions

We confirmed that the methodology designed to obtain pUBMh is highly reproducible and easy to apply. This biomaterial, when implemented under *in vitro* conditions, induces proliferation in fibroblasts, in macrophages the synthesis of proinflammatory cytokines such as MCP-1, TNF-α and IL-6 and is free of cytotoxicity in MSCs. While when used *in vivo* studies, it was shown that it allows the recruitment of polymorphonuclear and fibroblastoid cells from the host itself, which indicates that it could be an inducer of true tissue regeneration, free from inflammation of the surrounding tissues. This indicates that pUBMh is a scaffold that could be used free mixed with biomolecules or cells, inducing proliferation and allowing the complete regeneration and reparation of different tissues, which makes it an outstanding candidate for *in vivo* and preclinical studies.

Acknowledgements

The authors thank the Mexican company Fapsa Y Asociados S.A. De C.V. for donating the necessary bladders to carry out this important project.

Conflict of interest

No potential conflict of interest relevant to this article was reported.

Author contributions

GJG, AAH, JLG conducted laboratory tests; GRJG, AAH, JLG collected the data; MAM, RRP and MB analyzed the results; MAM, RRP and ESB conceived and designed the study; GRJG, AAH, JLG, MB and RRP wrote the manuscript; GSS and JGRM contributed to the final version of the manuscript. All authors read and approved the final manuscript.

References

[1] M. Qasim, D.S. Chae and N.Y. Lee, Advancements and frontiers in nano-based 3D and 4D scaffolds for bone and cartilage tissue engineering, *International Journal of Nanomedicine* **14** (2019), 4333.

[2] A. Ayala-Ham, J. Lopez-Gutierrez, M. Bermúdez, M. Aguilar-Medina, J.I. Sarmiento-Sánchez, C. López-Camarillo et al., Hydrogel-based scaffolds in oral tissue engineering, *Frontiers in Materials* **8** (2021), 708945.

[3] G.R. Jiménez-Gastélum, E.M. Aguilar-Medina, E. Soto-Sainz, R. Ramos-Payán and E.L. Silva-Benítez, Antimicrobial properties of extracellular matrix scaffolds for tissue engineering, *BioMed Research International* **2019** (2019), 9641456.

[4] F. Goker, L. Larsson, M. Del Fabbro and F. Asa'ad, Gene delivery therapeutics in the treatment of periodontitis and peri-implantitis: A state of the art review, *International Journal of Molecular Sciences* **20**(14) (2019), 3551.

[5] R. Sakata, T. Iwakura and A.H. Reddi, Regeneration of articular cartilage surface: Morphogens, cells, and extracellular matrix scaffolds, *Tissue Engineering Part B: Reviews* **21**(5) (2015), 461–473.

[6] K. Fukushima, M. Marques, T. Tedesco, G. Carvalho, F. Gonçalves, H. Caballero-Flores et al., Screening of hydrogel-based scaffolds for dental pulp regeneration—a systematic review, *Archives of Oral Biology* **98** (2019), 182–194.

[7] B.N. Cavalcanti, B.D. Zeitlin and J.E. Nör, A hydrogel scaffold that maintains viability and supports differentiation of dental pulp stem cells, *Dental Materials* **29**(1) (2013), 97–102.

[8] T. Vo, S. Shah, S. Lu, A. Tatara, E. Lee, T. Roh et al., Injectable dual-gelling cell-laden composite hydrogels for bone tissue engineering, *Biomaterials* **83** (2016), 1–11.

[9] S. Lu, J. Lam, J.E. Trachtenberg, E.J. Lee, H. Seyednejad, J.J. van den Beucken et al., Dual growth factor delivery from bilayered, biodegradable hydrogel composites for spatially-guided osteochondral tissue repair, *Biomaterials* **35**(31) (2014), 8829–8839.
[10] F. Gattazzo, A. Urciuolo and P. Bonaldo, Extracellular matrix: A dynamic microenvironment for stem cell niche, *Biochimica et Biophysica Acta* **1840**(8) (2014), 2506–2519.
[11] J.M. Aamodt and D.W. Grainger, Extracellular matrix-based biomaterial scaffolds and the host response, *Biomaterials* **86** (2016), 68–82.
[12] S.F. Badylak, The extracellular matrix as a biologic scaffold material, *Biomaterials* **28**(25) (2007), 3587–3593.
[13] L.T. Saldin, M.C. Cramer, S.S. Velankar, L.J. White and S.F. Badylak, Extracellular matrix hydrogels from decellularized tissues: Structure and function, *Acta Biomaterialia* **49** (2017), 1–15.
[14] G.R. Fercana, S. Yerneni, M. Billaud, J.C. Hill, P. VanRyzin, T.D. Richards et al., Perivascular extracellular matrix hydrogels mimic native matrix microarchitecture and promote angiogenesis via basic fibroblast growth factor, *Biomaterials* **123** (2017), 142–154.
[15] J. Soto-Sainz, E. Silva-Benítez, J. Romero-Quintana, A. Pozos-Guillen, E. Aguilar-Medina, A. Ayala-Ham et al., Synthesis and biofunctionalization of extracellular matrix hidrogel for bone regeneration, *Dental Materials* **1**(32) (2016), e31.
[16] J. Liang, P. Yi, X. Wang, F. Huang, X. Luan, Z. Zhao et al., Acellular matrix hydrogel for repair of the temporomandibular joint disc, *Journal of Biomedical Materials Research Part B: Applied Biomaterials* **108**(7) (2020), 2995–3007.
[17] J.L. Dziki, D.S. Wang, C. Pineda, B.M. Sicari, T. Rausch and S.F. Badylak, Solubilized extracellular matrix bioscaffolds derived from diverse source tissues differentially influence macrophage phenotype, *Journal of Biomedical Materials Research Part A* **105**(1) (2017), 138–147.
[18] D. Gong, F. Yu, M. Zhou, W. Dong, D. Yan, S. Zhang et al., *Ex vivo* and *in vivo* properties of an injectable hydrogel derived from acellular ear cartilage extracellular matrix, *Frontiers in Bioengineering and Biotechnology* **9** (2021), 740635.
[19] M. Kharaziha, A. Baidya and N. Annabi, Rational design of immunomodulatory hydrogels for chronic wound healing, *Advanced Materials* **33**(39) (2021), 2100176.
[20] S. Zhang, Y. Liu, X. Zhang, D. Zhu, X. Qi, X. Cao et al., Prostaglandin E2 hydrogel improves cutaneous wound healing via M2 macrophages polarization, *Theranostics* **8**(19) (2018), 5348.
[21] S. Jiang, S. Liu and W. Feng, PVA hydrogel properties for biomedical application, *Journal of the Mechanical Behavior of Biomedical Materials* **4**(7) (2011), 1228–1233.
[22] M.T. Spang and K.L. Christman, Extracellular matrix hydrogel therapies: *in vivo* applications and development, *Acta Biomaterialia* **68** (2018), 1–14.
[23] B. Xu, Y. Li, B. Deng, X. Liu, L. Wang and Q.L. Zhu, Chitosan hydrogel improves mesenchymal stem cell transplant survival and cardiac function following myocardial infarction in rats, *Experimental and Therapeutic Medicine* **13**(2) (2017), 588–594.
[24] B.N. Brown, R. Londono, S. Tottey, L. Zhang, K.A. Kukla, M.T. Wolf et al., Macrophage phenotype as a predictor of constructive remodeling following the implantation of biologically derived surgical mesh materials, *Acta Biomater.* **8**(3) (2012), 978–987.
[25] S.B. Cairo, J. Zhao, M. Ha and K.D. Bass, Porcine bladder extracellular matrix in paediatric pilonidal wound care: Healing and patient experience evaluation, *Journal of Wound Care* **28**(Sup5) (2019), S12–S19.
[26] E. Silva-Benítez, J. Soto-Sainz, A. Gordillo-Moscoso, H. Medellín-Castillo, J. Romero-Quintana, A. Pozos-Guillen et al., Designing a biofunctionalized extracellular matrix for bone regeneration, *Dental Materials* **30** (2014), e179.
[27] M.J. Sawkins, W. Bowen, P. Dhadda, H. Markides, L.E. Sidney, A.J. Taylor et al., Hydrogels derived from demineralized and decellularized bone extracellular matrix, *Acta Biomaterialia* **9**(8) (2013), 7865–7873.
[28] A. Ayala-Ham, M. Aguilar-Medina, J. León-Félix, J.G. Romero-Quintana, M. Bermúdez, J. López-Gutierrez et al., Extracellular matrix hydrogel derived from bovine bone is biocompatible *in vitro* and *in vivo*, *Bio-Medical Materials and Engineering* (2022), 1–14, Preprint.
[29] B.N. Brown, J.E. Valentin, A.M. Stewart-Akers, G.P. McCabe and S.F. Badylak, Macrophage phenotype and remodeling outcomes in response to biologic scaffolds with and without a cellular component, *Biomaterials* **30**(8) (2009), 1482–1491.
[30] J.T. Paige, M. Kremer, J. Landry, S.A. Hatfield, D. Wathieu, A. Brug et al., Modulation of inflammation in wounds of diabetic patients treated with porcine urinary bladder matrix, *Regen. Med.* **14**(4) (2019), 269–277.
[31] S. Chen, J. Shi, M. Zhang, Y. Chen, X. Wang, L. Zhang et al., Mesenchymal stem cell-laden anti-inflammatory hydrogel enhances diabetic wound healing, *Sci. Rep.* **5** (2015), 18104.
[32] S. Das, G. Singh, M. Majid, M.B. Sherman, S. Mukhopadhyay, C.S. Wright et al., Syndesome therapeutics for enhancing diabetic wound healing, *Adv. Healthc. Mater.* **5**(17) (2016), 2248–2260.
[33] M.T. Wolf, K.A. Daly, E.P. Brennan-Pierce, S.A. Johnson, C.A. Carruthers, A. D'Amore et al., A hydrogel derived from decellularized dermal extracellular matrix, *Biomaterials* **33**(29) (2012), 7028–7038.

[34] H.E. Desjardins-Park, D.S. Foster and M.T. Longaker, Fibroblasts and wound healing: An update, *Future Medicine* **15**(3) (2018), 491–495.
[35] G.W. Gibbons, Grafix®, a cryopreserved placental membrane, for the treatment of chronic/stalled wounds, *Advances in Wound Care* **4**(9) (2015), 534–544.
[36] J. Rožanc, L. Gradišnik, T. Velnar, M. Gregorič, M. Milojević, B. Vihar et al., Mesenchymal stem cells isolated from paediatric paravertebral adipose tissue show strong osteogenic potential, *Biomedicines* **10**(2) (2022), 378.
[37] B. Ugurlu and E. Karaoz, Comparison of similar cells: Mesenchymal stromal cells and fibroblasts, *Acta Histochemica* **122**(8) (2020), 151634.
[38] J.L. Spees, R.H. Lee and C.A. Gregory, Mechanisms of mesenchymal stem/stromal cell function, *Stem Cell Research & Therapy* **7**(1) (2016), 1–13.
[39] W.M. Jackson, L.J. Nesti and R.S. Tuan, Mesenchymal stem cell therapy for attenuation of scar formation during wound healing, *Stem Cell Research & Therapy* **3**(3) (2012), 1–9.
[40] C.C. Yates, M. Rodrigues, A. Nuschke, Z.I. Johnson, D. Whaley, D. Stolz et al., Multipotent stromal cells/mesenchymal stem cells and fibroblasts combine to minimize skin hypertrophic scarring, *Stem Cell Research & Therapy* **8**(1) (2017), 1–13.
[41] Y. Fu, X. Fan, C. Tian, J. Luo, Y. Zhang, L. Deng et al., Decellularization of porcine skeletal muscle extracellular matrix for the formulation of a matrix hydrogel: A preliminary study, *J. Cell. Mol. Med.* **20**(4) (2016), 740–749.
[42] I. Pineau and S. Lacroix, Proinflammatory cytokine synthesis in the injured mouse spinal cord: Multiphasic expression pattern and identification of the cell types involved, *Journal of Comparative Neurology* **500**(2) (2007), 267–285.
[43] J.R. Bethea, H. Nagashima, M.C. Acosta, C. Briceno, F. Gomez, A.E. Marcillo et al., Systemically administered interleukin-10 reduces tumor necrosis factor-alpha production and significantly improves functional recovery following traumatic spinal cord injury in rats, *Journal of Neurotrauma* **16**(10) (1999), 851–863.
[44] H. Beyer and M. Stanley, Tumor necrosis factor-alpha increases hepatic DNA and RNA and hepatocyte mitosis, *Biochemistry International* **22**(3) (1990), 405–410.
[45] K. Mealy and D. Wilmore, Tumour necrosis factor increases hepatic cell mass, *British Journal of Surgery* **78**(3) (1991), 331–333.
[46] P. Akerman, P. Cote, S.Q. Yang, C. McClain, S. Nelson, G. Bagby et al., Antibodies to tumor necrosis factor-alpha inhibit liver regeneration after partial hepatectomy, *American Journal of Physiology-Gastrointestinal and Liver Physiology* **263**(4) (1992), G579–G585.
[47] G. Arderiu, E. Peña, R. Aledo, S. Espinosa and L. Badimon, Ets-1 transcription is required in tissue factor driven microvessel formation and stabilization, *Angiogenesis* **15**(4) (2012), 657–669.
[48] Y. Hayashi, M. Murakami, R. Kawamura, R. Ishizaka, O. Fukuta and M. Nakashima, CXCL14 and MCP1 are potent trophic factors associated with cell migration and angiogenesis leading to higher regenerative potential of dental pulp side population cells, *Stem Cell Research & Therapy* **6**(1) (2015), 1–19.
[49] K.H. Hong, J. Ryu and K.H. Han, Monocyte chemoattractant protein-1–induced angiogenesis is mediated by vascular endothelial growth factor-A, *Blood* **105**(4) (2005), 1405–1407.
[50] J. Li, A.J. Bower, V. Vainstein, Z. Gluzman-Poltorak, E.J. Chaney, M. Marjanovic et al., Effect of recombinant interleukin-12 on murine skin regeneration and cell dynamics using *in vivo* multimodal microscopy, *Biomedical Optics Express* **6**(11) (2015), 4277–4287.
[51] A. Das, M. Sinha, S. Datta, M. Abas, S. Chaffee, C.K. Sen et al., Monocyte and macrophage plasticity in tissue repair and regeneration, *The American Journal of Pathology* **185**(10) (2015), 2596–2606.
[52] K. Výborný, J. Vallová, Z. Kočí, K. Kekulová, K. Jiráková, P. Jendelová et al., Genipin and EDC crosslinking of extracellular matrix hydrogel derived from human umbilical cord for neural tissue repair, *Scientific Reports* **9**(1) (2019), 1–15.
[53] J. Xue, B. Feng, R. Zheng, Y. Lu, G. Zhou, W. Liu et al., Engineering ear-shaped cartilage using electrospun fibrous membranes of gelatin/polycaprolactone, *Biomaterials* **34**(11) (2013), 2624–2631.
[54] L. Teodori, A. Costa, R. Marzio, B. Perniconi, D. Coletti, S. Adamo et al., Native extracellular matrix: A new scaffolding platform for repair of damaged muscle, *Frontiers in Physiology* **5** (2014), 218.
[55] E.P. Brennan, J. Reing, D. Chew, J.M. Myers-Irvin, E.J. Young and S.F. Badylak, Antibacterial activity within degradation products of biological scaffolds composed of extracellular matrix, *Tissue Engineering* **12**(10) (2006), 2949–2955.